Reprinted from Preprint Volume: 10th Conference on Weather Forecasting & Analysis, June 25-29, 1984, Clearwater Beach, Fla. Published by the American Meteorological Society, Boston, Mass.

4.5 WEIGHTING FUNCTION PARAMETERS FOR OBJECTIVE INTERPOLATION OF METEOROLOGICAL DATA

By

F. Caracena, S. L. Barnes, and C. A. Doswell III
NOAA/ERL/WRP - Boulder, Colorado 80303

## 1. INTRODUCTION

Interpolation using the weighted average method is a handy way of simultaneously smoothing and reformatting irregularly spaced data onto a regular grid where it can be used for model inputs or further computations. Cressman (1959) called the technique "objective analysis." The process in this paper is simply called interpolation.

Interpolation variously performed can result in a wide range of outputs all based on the same input data. The form of the weighting function is one source of variability, and the choice of weighting function parameters is another. This raises two important questions: (1) how can the weighting function be chosen, and (2) can the choice of weighting function parameters be optimized?

The answer to these two questions is rather involved and really beyond the scope of this report. Instead, consider these discussions as a point of departure for later addressing much larger issues. They are rather specialized: a Gaussian weighting function has been used, and most of the arguments have been restricted to one dimensional cases. However, the conclusions represent results which can be used in practical applications.

The reader may find some of the following discussion (particularly in Section 3) somewhat abstract. It is necessarily presented here because the conclusions follow directly from these abstract discussions. If the discussion seems too abstract, simply skip over it; but be sure to read the conclusions and examples. These will be elaborated on at the conference, but the theory will be presented only here.

## 2. THE GAUSSIAN WEIGHTING FUNCTION

One of the many choices presented by an interpolation scheme is in selecting the weighting function. In general interpolation scheme can be stated in terms of two equations:

$$f_{ij} = \sum_{s=1}^{N} w(D_{ijs})\, F(x_s) , \qquad (1)$$

$$i = 1, 2, .., N_x, \; j = 1, 2, .., N_y$$

$$\sum_{s=1}^{N} w(D_{ijs}) = 1 . \qquad (2)$$

The index s in (1) and (2) refers to the set of input data points and the two indices i, j, refer to the set of output points which are located on a regular grid on a surface. The weighting function w is an analytic function of $D_{ijs}$ the distance between an output grid point (indexed by i and j) and an input data point (index by s). The sampled value of the otherwise unknown function at the point $x_s$ is represented by $F(x_s)$, and the interpolated value at the grid point (indexed by ij) is represented by $f_{ij}$.

The interpolation procedure used in this paper is based on a Gaussian weighting function as proposed and described by Barnes (1964). The weighting function must also satisfy the normalization (2), and is therefore defined as follows:

$$w(\lambda_o, D_{ijs}) = \exp(-D_{ijs}^2/\lambda_o^2)/\left[\sum_{s'=1}^{N} \exp(-D_{ijs'}^2/\lambda)\right] . \qquad (3)$$

The parameter, $\lambda_o$, sets the approximate range of influence, which is also a smoothing scale length. The form of the weighting function (3) assumes that the data points are distributed along both the x and y axis with about the same spacing. If this is not the case, then there must be a separate scale parameter for each axis.

At first sight, the weighting function given by (3) might appear to depart significantly from a Gaussian because of division by the normalizing sum. This is not the case, however, because this sum is almost a constant over the input data domain under certain conditions, and departs significantly from a constant value only beyond the boundaries of this domain. This is demonstrated by the plot in Fig. 1a of the normalizing sum over the right half of a regularly spaced 11 point interval on a straight line using a Gaussian weighting function parameter of $\lambda_o = 1.4$. The normalizing sum is progressively closer to a constant as the parameter $\lambda_o$ becomes progressively greater than the average data separation. Over the interior of a two dimensional data domain, this sum can also approximate a constant, and likewise falls off rapidly from this constant value beyond the boundaries the two dimensional domain. An example of this value is presented in Fig. 1b which shows the number of data points influencing a particular interpolation over the U.S. radiosonde grid.

As a result of the behavior of the sum of the weights (Fig. 1a and 1b), the weighting functions (3) for points inside the data domain will be almost identically Gaussian (see Fig. 2a), but for the boundary points will depart radically from the Gaussian form. Further, the boundary points will have weighting functions that are very close to Gaussian on those portions facing inward toward the interior of the data domain, but radically different from Gaussian in the outward facing portions. This behavior is illustrated by the plots in Fig. 2b where 5 weighting functions over half the inter-

val (from Fig. 2a) are translated and superposed relative to a common center. The effect of a asymmetric weighting functions is a distortion in the interpolated values near the boundaries and beyond. The tendency of the interpolated field tends to flatten out and approach the value of the boundary points asymptotically. This distortion also extends inward from the boundaries about one scale length, $\lambda_o$.

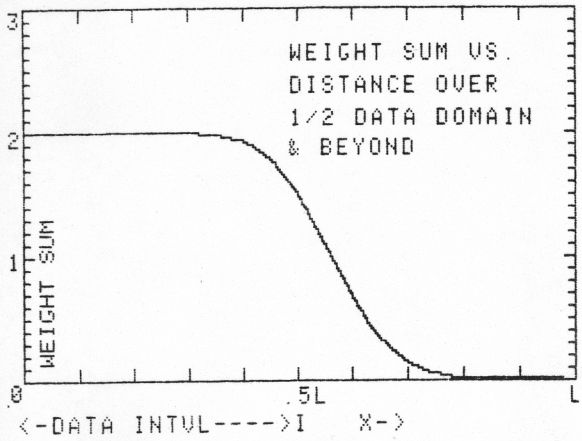


Fig. 1a. Plot of normalizing sum of Gaussian weights for the positive half of sample interval consisting of 11 uniformly spaced data points along the x axis symmetrically distributed about the origin.

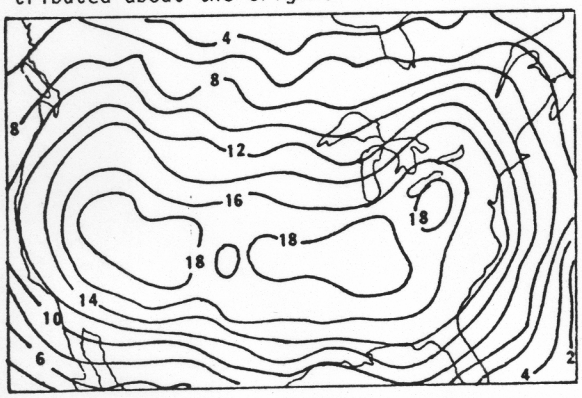


Fig. 1b. Smoothed distribution of the number of data affecting the calculation of the interpolated value at each grid point for the U.S. radiosonde grid (From Barnes, 1964).

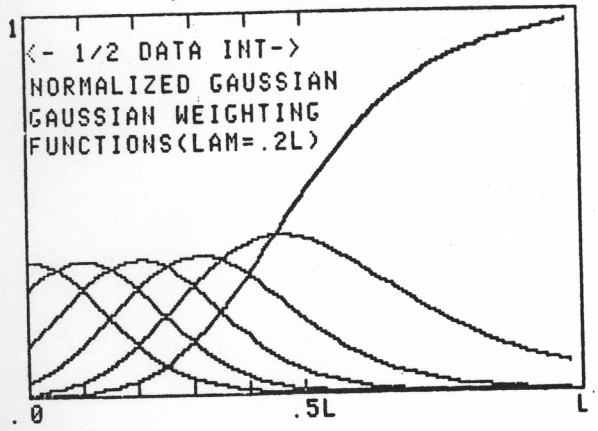


Fig. 2a. Plot of 6 weighting functions corresponding to situation described in 1a.

## 3. DISCUSSION OF ERRORS ASSOCIATED WITH SAMPLING INTERPOLATION AND SMOOTHING

The effects of finite, discrete sampling of a function are usually discussed in communications and information theories. Fourier transform theory and harmonic analysis usually play a central role in these discussions. The following discussion is a very brief summary of that portion of the one dimensional theory which is used in discussing interpolation and sampling errors.

The Fourier transform ($F_{ft}$) of a function (F) in one dimension is given by the expression,

$$F_{ft}(k) = \int_{-\infty}^{\infty} dx\, e^{ikx} F(x) , \qquad (4a)$$

where k is the wave number,

$$k = 2\pi/\lambda . \qquad (5)$$

The inverse Fourier transform is defined as:

$$F(x) = \frac{1}{2\pi} \int_{-\infty}^{\infty} dk\, e^{-ikx} F_{ft}(k) . \qquad (4b)$$

The convolution of two functions is another central concept of information theory,

$$H(x) = \int_{-\infty}^{\infty} dx' F(x - s') G(x') . \qquad (6)$$

The Fourier transform and the convolution are related by the Convolution Theorem which states:

a. the Fourier transform of the convolution of two functions is equal to the product of their Fourier transforms, and

b. the Fourier transform of the product of two functions is equal to the convolution of their Fourier transforms.

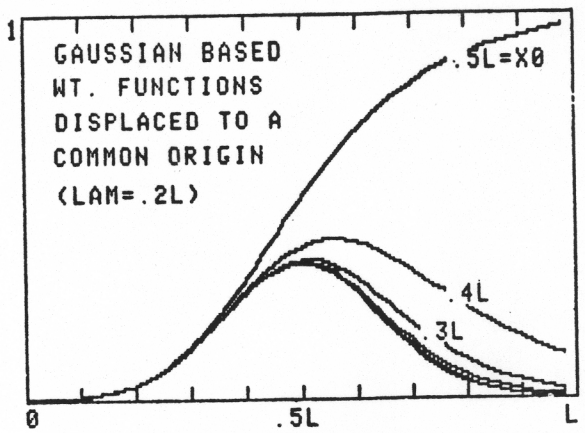


Fig. 2b. Plot of same 6 weighting functions in Fig. 2a but with centers translated so that they coincide.

For example, the Fourier transform of the convolution (6) is

$$H_{ft}(k) = F_{ft}(k)\, G_{ft}(k) \ . \qquad (7)$$

Alternatively, the Fourier transform of the product,

$$h(x) = f(x)\, g(x) \ , \qquad (8)$$

is

$$h_{ft}(k) = \int_{-\infty}^{\infty} dk'\, f_{ft}(k - k')\, g_{ft}(k') \ . \qquad (9)$$

The concept of a Fourier transform is important in information theory because it characterizes the information content of the data. When the signal is concentrated in a narrow range of wavelengths, the Fourier transform is narrow, but the spatial pattern is relatively smooth. Conversely, a broad Fourier transform implies that the signalal is spread over many wavelengths, so the spatial pattern has a lot of variation. The details of Fourier analysis are complex, but the interested reader will find them well worth the effort (see, e.g. Champeney, 1973).

The convolution theorem is an important tool because it allows one to evaluate rather involved Fourier transforms. Specifically, in our application we wish to know what happens to the Fourier transform of a function as it is sampled over restricted domains. Consider the Fourier transform of a continuous function that is sampled continuously over a limited spatial domain, $-L/2 \leq x \leq L/2$. This can be represented by the product,

$$F'(x) = R(x)\, F(x) \ , \qquad (10)$$

where R is the rectangular function,

$$R(x) = \begin{cases} 1 & , -L/2 \leq x \leq L/2 \ , \\ 0 & , \text{otherwise} \ . \end{cases} \qquad (11)$$

The sampled function F'(x) in (10) is identical to F(x) over the restricted domain specified by R(x) and is zero elsewhere. The Fourier transform of the product (10) can be evaluated with the convolution theorem to yield the following:

$$F'_{ft}(k) = \int_{-\infty}^{\infty} dk'\, R_{ft}(k - k')\, F_{ft}(k') \ . \qquad (12)$$

The Fourier transform of the rectangular function (11) is readily evaluated to be the following:

$$R_{ft}(k) = 2 \sin (k\, L/2)/k \ . \qquad (13)$$

Note that there is a symmetry between Fourier transform and its inverse. Together these constitute what is known as a "Fourier transform pair." For example, a spatial function which is the analog of (13),

$$s(x) = 2 \sin (k_o\, x/2)/x \ , \qquad (14)$$

has a Fourier transform that is the analog of (11),

$$S_{ft}(k) = \begin{cases} 1 & , -k_o/2 \leq x \leq k_o/2 \ , \\ 0 & , \text{otherwise} \ . \end{cases} \qquad (15)$$

The function (14) has a Fourier spectrum which cuts off sharply outside the band defined by the limits $\pm k_o/2$, and so is called a "band-limited" function.

Now suppose the function (14) is sampled over the interval $-L/2 \leq x \leq L/2$. In this case the sample function has a Fourier transform which is given by (12) with the Fourier transform function $S_{ft}$ replacing $F_{ft}$. The resultant transform, for a spectral distribution $S_{ft}$ which is ten times as wide as $R_{ft}$, is shown in Fig. 3a. The Fourier transform of the sampled function is in this case a fairly good approximation to the source function (15). When the source function has a Fourier spectrum $S_{ft}$ that is

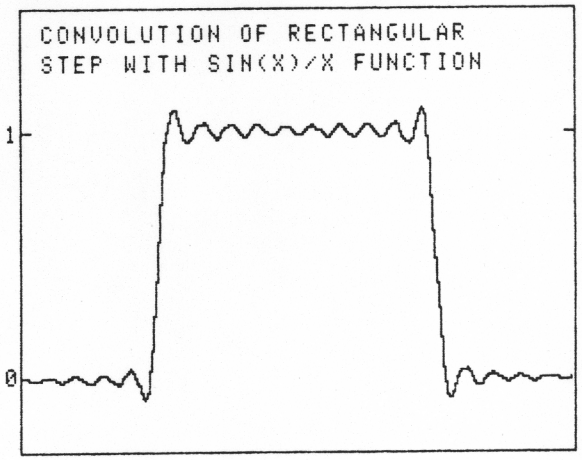


Fig. 3a. The Fourier transform of the product of the band limited function (14) and the rectangular function (11) where the spectral width of the sampled function (15) is ten times wider than that of the rectangular function (13).

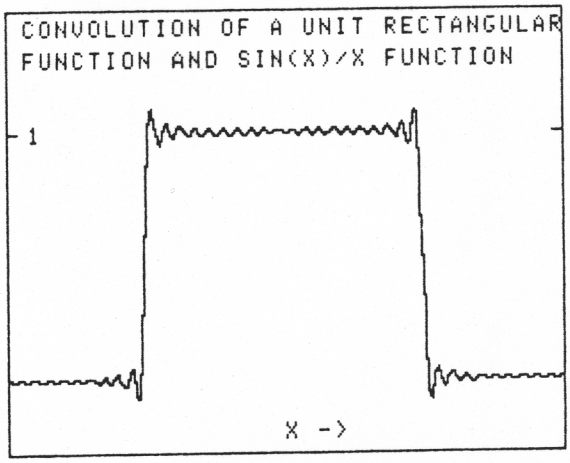


Fig. 3b. Same as Fig. 3a but with a spectral width for the source function twenty times wider than that of the rectangular function.

twenty times wider that $R_{ft}$, the convolution (12) gives a still better approximation of the actual Fourier transform of the source function (see Fig. 3b).

In general, as the band width of $F_{ft}$ in (12) is progressively wider than that of $R_{ft}$, the closer the convolution of them, $F'_{ft}$, approximates the Fourier transform of the source function. In terms of the spatial counterparts, this means that observed features progressively suffer less distortion as more and more of their environment is sampled. This means that a meteorological network should be able to sample an area which is about an order of magnitude larger in linear dimensions than the phenomenon of interest in order to avoid this distortion.

Discrete sampling of a function over a finite domain, $-L/2 \leq x \leq L/2$ in one dimension, produces effects analogous to those discussed above, but with additional complexities. Here, only the effects of sampling on a regular grid are considered because the complexity of irregular sampling is beyond the scope of this discussion. The discussions here apply to irregular sampling but with some modifications to be addressed in a future publication.

Consider the weighting function interpolation scheme (1), (2), (3). This procedure, although discrete, can be written in the form of an integral,

$$f(x) = \int_{-\infty}^{\infty} dx'\, w(\lambda_o, |x - x'|)\, F(x')\, \Delta(x') , \qquad (16)$$

with the help of the Dirac comb function

$$\Delta(x) = \sum_{s=o}^{N-1} \delta(x - x_s) . \qquad (17)$$

The function, f(x), is the interpolated value of the sampled function, F(x). The weighting function in (16) is the one dimensional form of (3) with the added feature that the normalizing sum is taken to be constant so that

$$w(\lambda_o\ |x - x'|) \simeq \text{cons}^*\exp[-(x - x')^2/\lambda_o^2] . \qquad (18)$$

The previous section shows that this sum is well approximated by a constant for the interior points of the sample interval when N = 11, while it departs significantly from a constant only at the two end points and beyond.

The Fourier transform of the interpolated function in (16) is computed by repeated applications of the convolution theorem. The first application yields,

$$f_{ft}(k) = w_{ft}(\lambda_o, k)\, [F\Delta]_{ft}(k) , \qquad (19)$$

where the convolution of the weighting function is

$$w_{ft}(\lambda_o, k) = \text{const}^*\exp[-(k\lambda_o/2)]^2 . \qquad (20)$$

The second application of the convolution theorem yields the Fourier transform of the product on the right hand side of (19),

$$\{F\Delta\}_{ft}(k) = \int_{-\infty}^{\infty} dk'\, F_{ft}(k')\, \Delta_{ft}(k - k') . \qquad (21)$$

In evaluating the Fourier transform, $\Delta_{ft}$, assume that the points $x_s$ in (17) are regularly spaced on a straight line,

$$x_s = [s - (N - 1)\, N/2]\, \Delta x , \qquad (22)$$

where the sample interval, $\Delta x$, width of the sample domain, L, and number of samples, N, are related by

$$(N - 1)\, \Delta x = L . \qquad (23)$$

With (22) and (23) the Fourier transform (4a) of (17) is evaluated in a straightforward manner yielding,

$$\Delta_{ft}(k) = \sum_{n=o}^{N} \exp[ik\,(n - \tfrac{N-1}{2})\, \Delta x] . \qquad (24)$$

Champeney (1973) writes (24) in the analytically more compact form

$$\Delta_{ft}(k) = \sin(kN\Delta x/2)/\sin(k\Delta x/2) . \qquad (25)$$

This function (25) is plotted in Fig. 4, which shows that $\Delta_{ft}$ is periodic in k with a fundamental period $2\pi/\Delta x$. The central major spike in each fundamental cycle has a width of $4\pi/[N\Delta x]$.

Consider what happens to (25) as the number of samples within the interval, L, approaches infinity and the distance between nearest samples, $\Delta x$, correspondingly approaches zero according to (23). In this case the interval weighted Fourier transform (25) has a well defined limit,

$$\lim_{\substack{N \to \infty \\ \Delta x \to 0}} \Delta_{ft}(k)\, \Delta x = 2 \sin(kL/2)/L , \qquad (26)$$

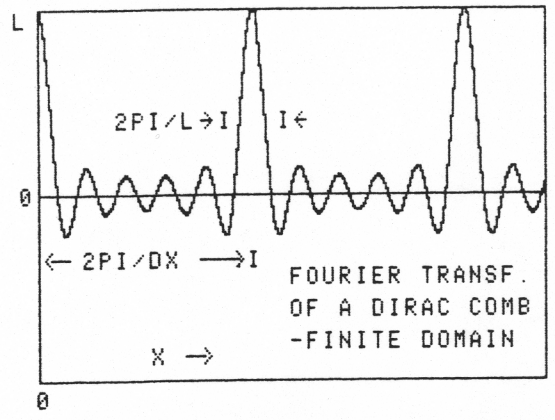


Fig. 4a. A plot of the Fourier transform (25) of the finite Dirac comb (17). It is periodic with a wave number periodicity of $2\pi/2\Delta x$, and the width of its major peaks is $4\pi/(N\,\Delta x)$.

which is identical to the Fourier transform (13) of the rectangular function (11). Thus, the periodic function (25) consists a fundamental, repeating pattern which approaches the Fourier transform of a rectangular function (11) as the sampling density increase, while the major side lobes of this function are displaced further to the sides.

An example of how well the Fourier transform of the Dirac comb (22) with eleven sample points approximates that of a rectangular function (13) is seen in Fig. 5, where these two functions are superimposed. The central spike makes an almost perfect fit, and the lesser side peaks progressively are poorer approximations until the main side lobes are reached.

Given the above properties, it is possible to gain some understanding of the Fourier transform of the product of a Dirac comb with that of the sampled function (21). Suppose the bandwidth of the sampled function is simultaneously much less than twice the Nyquist wave number ($2\pi/\Delta x$) and much greater than the width of the major peaks in the Fourier transform of the Dirac comb function ($4\pi/(N\,\Delta x]$). The resulting effect of the convolution is to generate a periodic function, the central peak (centered on the origin) of which approximates the Fourier transform of the sampled function. The remaining periods to $\pm\infty$ represent spurious repetition of the spectrum due to discrete sampling. Depending on the sharpness of the band limits, the central period of this pattern then contains very little contamination due to contributions from the repacted portions of the spectrum.

This contamination is called non-local aliasing. The effects of both types of aliasing are illustrated in Fig.'s 6a-d where the convolutions of $\Delta_{ft}(k)$ with four rectangular functions (of extent $\Delta k$ = 2, 3, 4, 5) are plotted. Notice how local aliasing increases until it becomes non-local, as the spectral width of the source function approaches the separation of major lobes in the Fourier transform of the Dirac comb.

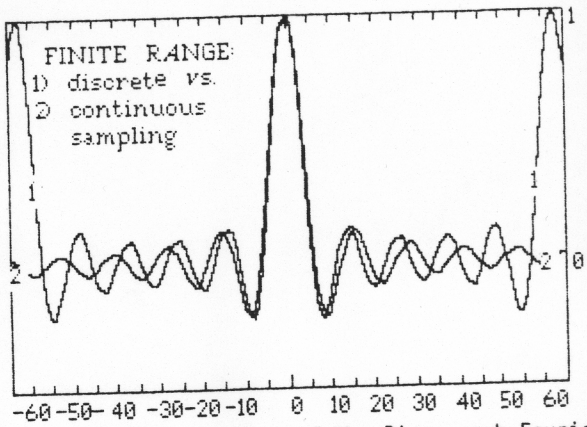


Fig. 5. Superportion of the Dirac comb Fourier transfor with the Fourier transform of a rectangular function that spans the data interval.

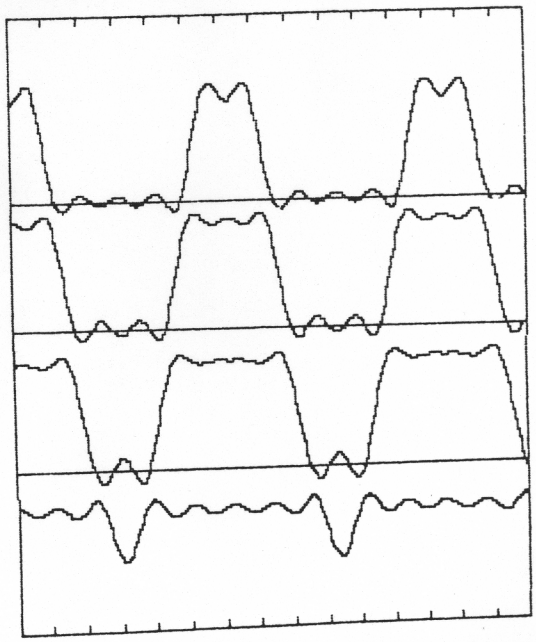

Fig. 6. A series of convolutions with the Dirac comb Fourier transform (see Fig. 5 and Eq. 22) with a series of rectangular spectral distributions of progressively broader extent which from top to bottom they are $\Delta k$ = 2, 3, 4, 5.

## 4. DISCUSSION OF APPLICATIONS

There are two sources of error which are associated with interpolating over a limited domain. First, there is a truncation of the sample function due to the finite domain size. To eliminate this type of error one must make the data domain about an order of magnitude larger than the phenomenon being sampled. Second, there is a more serious source of error in the edge effect. Weighted average interpolation produces an edge distortion that extends inwards from the boundaries of the data domain about one smoothing scale-length.

The edge distortion due to finite domain size can be reduced to a negligible amount if the analysis domain is one scale-length smaller in linear dimensions than the data domain. A corollary of this rule is that the number of data samples must be large enough to allow for a significant analysis area. For example, with a network of 9 stations there is no area that escapes significant edge distortion. In fact, 25 quasi-uniformly distributed stations, are required to just begin to give a meaningful analysis. With this minimum number, there is an undistorted analysis area of only about $2\Delta x$ by $2\Delta y$.

Discrete sampling produces additional types of error over and above those associated with the finite size of the data domain. The principal source of error is a folding of the Fourier components or "aliasing" (Blackman and Tukey, 1958). Aliasing error, in principle, can be reduced to negligible size through two procedures: (1) make the sample interval $\Delta x$ small enough that it is smaller than any significant wave length (or feature) in the phenomenon that is being sampled, and (2) choose a smoothing scale length $\lambda_o$ in the weighting function that gets rid of the aliasing that remains without destroying significant parts of the signal.

Aliasing due to significant power at wavelengths at or below the $2\Delta x$ level has a patho-

logical effect on interpolation. If the bandwidth of the source function is larger than the Nyquist frequency, $2\pi/2\Delta x$, then the interpolated field has a Fourier spectrum that is contaminated by aliasing from side lobes. The noise from this non-local aliasing cannot be removed by smoothing and therefore it seriously distorts the interpolated field. The only way to overcome non-local aliasing is to sample the phenomenon with sample intervals ($\Delta x$, $\Delta y$) that are smaller than half the least significant wave length.

Even if the source function is sampled sufficiently, there remains another component of aliasing which can be removed by smoothing. A discretely sampled function, with an appropriate sample interval, has a periodic Fourier transform. The spectrum consists of a central lobe (about k = o) which is duplicated to infinity in all directions with a periodicity which is twice the Nyquist frequency ($2\pi/\Delta x$). However, only the central lobe contains the signal, while the side lobes represent various components of noise. Since the function was sampled sufficiently, the central lobe contains no significant aliasing error and therefore, this aliasing error can be removed simply by suppressing all the side lobes.

This suppression is accomplished through proper choice of smoothing parameter in the weighting function. This is due to the fact that the spectrum of the interpolated function is given by the product of the Fourier transform of the weighting function and that of the sample function. The Fourier transform of the weighting function (18) is approximately the Gaussian function,

$$G_{ft}(k) = \text{const}*\exp[-(k\lambda_o/2)^2] \qquad (27).$$

Now, the parameter $\lambda_o$ in (27) can be chosen such that the side lobes appear with less than any specified percentage of the amplitude of the central lobe. To do this, simply set the half width (at the specified level) of (27) to the Nyquist interval and set the response of the weighting function (27) equal to a specified tolerance ($\varepsilon$) as follow:

$$\exp\left[-\left(\frac{2\pi}{2\Delta x}\frac{\lambda o}{2}\right)^2\right] \leq \varepsilon \qquad (28)$$

Solving the inequality (28) for the smoothing parameter, $\lambda_o$, we get,

$$\lambda_o \geq \frac{2\Delta x}{\pi} \; -\ln(\varepsilon) \qquad (29).$$

The relation (29) specifies the smoothing scale length necessary to reduce the nearest side lobes to at least $\varepsilon$ of the amplitude of the central lobe. If for example, we specify, $\varepsilon \geq 0.01$ then we must smooth by an amount $\lambda_o \geq 1.366\,\Delta x$.+ Or we can relate the requirement to $\varepsilon$ = 0.1, in which case we can use the smaller scale smoothing parameter, $\lambda_o \geq 0.966\Delta x$.

The results of the previous discussion about aliasing can be reduced to a simple rule: choose the smoothing parameter in the weight function to be about the same size, or slightly larger than, the average sample interval of the data. At this level of smoothing, the contamination due to aliasing is held to less than 10% of the true signal. However, the smoothing should not be too strong, or else a significant amount of the signal may be attenuated, and a significant portion of the interpolated values near the boundaries may be distorted by edge effect. Therefore the smoothing parameter should not be too much greater than about $1.4\Delta x$.

## 5. EXAMPLES

The results of the foregoing discussions are applied to two examples on a two dimensional plan: the first is an analytic test pattern, and the second is extracted from an actual meteorological case study. Both examples employ Gaussian interpolation with but a single pass, since the effect of multiple passes is beyond the scope of this paper.

Example 1. The test pattern plotted in Fig. 7 was generated by the function,

$$Z(x,y) = -100\sin(0.2\pi x)\sin(0.2\pi y) . \qquad (30)$$

This function was sampled at 81 points, the x, y coordinates of which were chosen initially on a regular grid ($\Delta x$, $\Delta y$ = 1.375 units) and then pseudo-random values between the limits ±25% the original spacing were added to these coordinates. The original sample range was 0-11 for both x and y coordinates and was broadened slightly by the randomizing procedure.

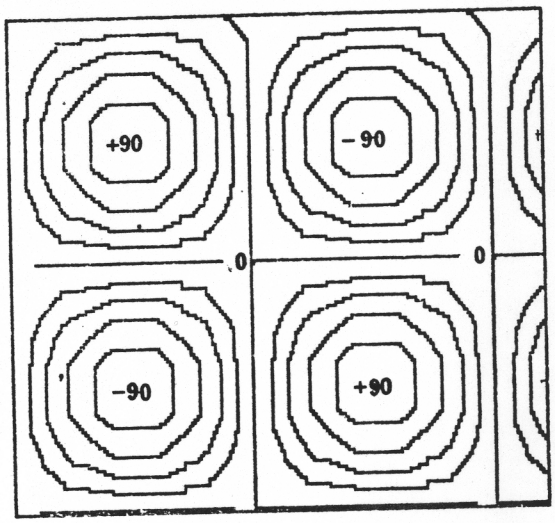


Fig. 7. A contour representation of the original test function $Z(x,y) = -\sin(.2\pi x)\sin(.2\pi y)$. The contours extend from a lowest value of -80 to a heighest value of +80, and the contour interval is 20.

+Note that in this case $\Delta x$ is the average sample interval and not the grid interval of the interpolated field.

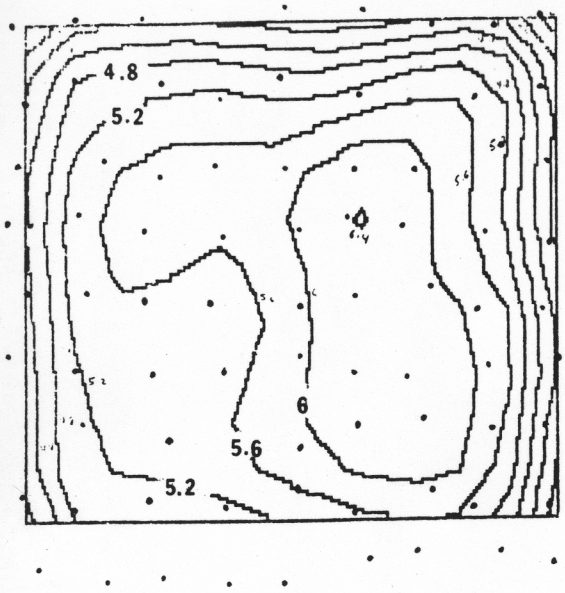


Fig. 8. A contour presentation of the sum of the Gaussian weights at points within the analysis domain. The heighest contour in the upper, right, central portion of the figure is 6.4 and the lowest contour in the upper righthand corner is 3.2. The contour in Ferval is 0.4.

As a result of randomizing, the normalizing sum is not strictly constant over the interior of the data domain but varies weakly there (see Fig. 8). Its behavior is similar to that of the radiosonde grid depicted in Fig. 1b. Notice in Fig. 8 the lack of a strong gradient in the weighting sums at the bottom of the figure. This happens because the analysis domain is shifted approximately one smoothing scale length up from the data boundary.

The effects of varying the smoothing length ($\lambda_o$) on single-pass Gaussian interpolation are apparent in the series of figures (Figs. 9a-9c). At $\lambda_o = 0.365\ \Delta x$ (Fig. 9a) the smoothing length is well below its opimal value for one dimension ($\lambda_o = 1.366$), and note that it is heavily contaminated by aliasing. However, the edge distortion is not significant because of the smallness of the smoothing parameter in relation to the grid size.

Notice that there is a progressive improvement in the quality of the interpolated field as the smoothing parameter approaches the one dimensional optimal value (Figs. 9a-9c). True to the foregoing theoretical discussions, the value $\lambda_o = 1.366\ \Delta x$ (see Fig. 10d) represents about the best compromise in simultaneously minimizing the distortion, due to aliasing and edge effects. As the smoothing length is increased beyond the optimal value, aliasing is further reduced but there is also a significant decrease in fidelity owing to loss in response and edge distortion (see Fig. 9c).

Fig. 9. A series of Gaussian weighted sum interpolations with progressively more smoothing:

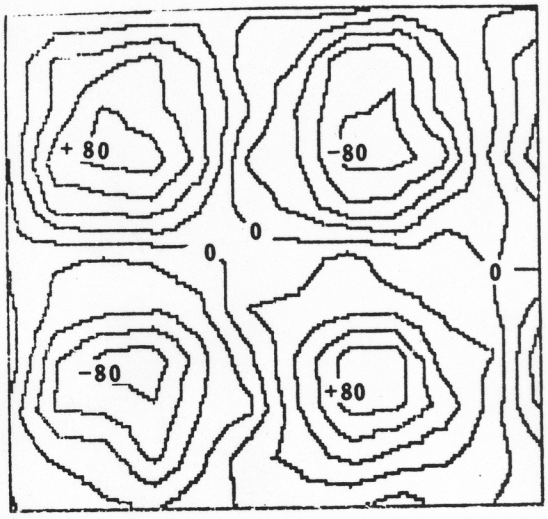


Fig. 9a. $\lambda_o = 0.365\ \Delta x$,

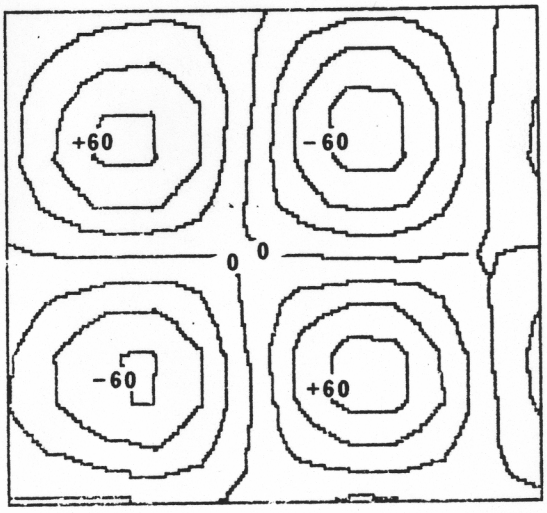


Fig. 9b. $\lambda_o = 1.366\ \Delta x$,

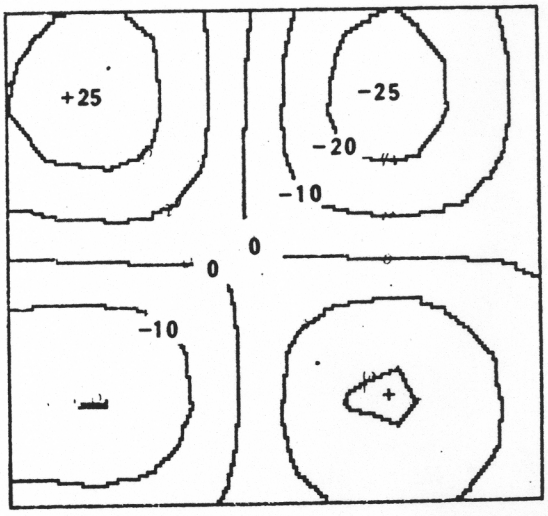


Fig. 9c. $\lambda_o = 2.18\ \Delta x$,

Fig. 10. A series of Gaussian weighted interpolations of 700-300 thickness for 1200 GMT, 25 June 1982 with progressively stronger smoothing:

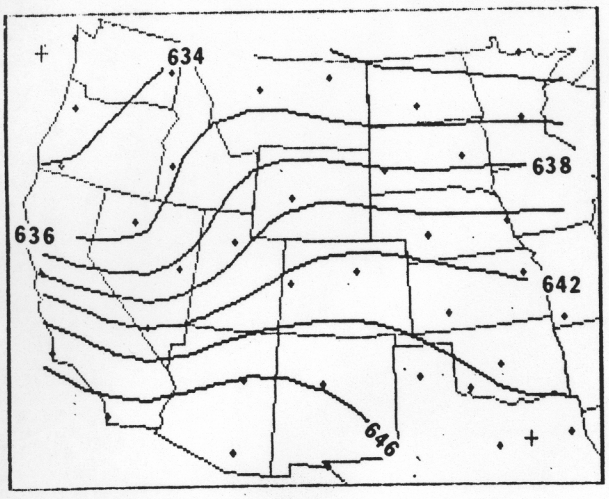


Fig. 10a. $\lambda_o$ = 500 km,

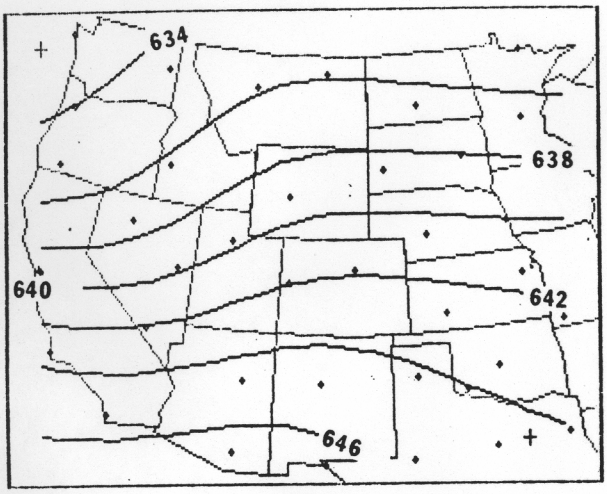


Fig. 10b. $\lambda_o$ = 750 km, and

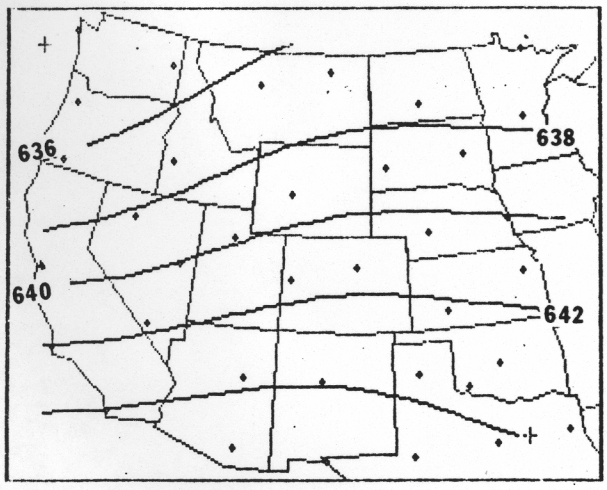


Fig. 10c. $\lambda_o$ = 1000 km.

Example 2. The same effects described above are all apparent in the three analysis of the 700-300 mb thickness field for 1200 GMT, 25 June 1982 (Figs. 10a-c). However in this case, there is no known function against which to compare the results. Since the first analysis (Fig 10a) has a smoothing parameter which is closest to the ideal smoothing length, it represents the best analysis in the series. It has the least noise contamination and edge effects. The other two analyses (Figs. 10b and 10c) progressively flatten the field and contaminate it with edge distortion.

## 6. CONCLUSION

This paper has presented a discussion of how aliasing, smoothing and edge effects affect the values of an interpolated field. The ideas used here are extensions of those used in information theory which was developed in connection with electrical signal processing. Unlike our colleagues in the electronic field, however, meteorological "signals" are not sampled as often as desired nor on an arbitrarily detailed grid. In fact, the situation usually confronting us is a sample that is just barely adequate to accomplish our analysis.

The result is that we must exercise special care to see if (1) a meaningful analysis is possible, (2) smooth sufficiently to discard aliased noise, and (3) not oversmooth lest edge effects and loss of information also deteriorate the output.


## 7. *Acknowledgements*

*We would like to thank Mrs. Sandra Chandler for her patience and expert typing.*


## 8. REFERENCES


Barnes, S.L., 1964: A technique for maximizing details in numerical weather map analysis. J. Appl. Meteor., 3, 396-409.

Barnes, S.L., 1973: Mesoscale objective maps analysis using weighted time-series observations. NOAA Tech. Memo. ERL NSSL-62, 60 pp.

Blackman, R.B. and J.W. Tukey, 1958: The Measurement of Power Spectra. Dover Publications, Inc., New York, 190 pp.

Champeney, D.C., 1973: Fourier Transforms and Their Physical Applications. Academic Press, London, New York, 250 pp.

Cressman, G.P., 1959: An operational objective analysis system. Mon. Wea. Rev., 87, 367-374.